Published in final edited form as:
*Cancer Res*. 2011 July 15; 71(14): 4857–4865. doi:10.1158/0008-5472.CAN-11-0455.

# The Mef/Elf4 transcription factor fine tunes the DNA damage response

**Goro Sashida**[1], **Narae Bae**[1], **Silvana Di Giandomenico**[1], **Takashi Asai**[1], **Nadia Gurvich**[1], **Elena Bazzoli**[1], **Yan Liu**[1], **Gang Huang**[1], **Xinyang Zhao**[1], **Silvia Menendez**[1], and **Stephen D Nimer**[1]

[1]Molecular Pharmacology and Chemistry Program of the Sloan-Kettering Institute, Memorial Sloan-Kettering Cancer Center, New York, NY 10065

## Abstract

The ATM kinase plays a critical role in initiating the DNA damage response that is triggered by genotoxic stresses capable of inducing DNA double strand breaks. Here, we show ELF4/MEF, a member of the ETS family of transcription factors, contributes to the persistence of γH2AX DNA damage foci, and promotes the DNA damage response leading to the induction of apoptosis. Conversely, the absence of Elf4 promotes the faster repair of damaged DNA and more rapid disappearance of γH2AX foci in response to γ-irradiation, leading to a radio-resistant phenotype despite normal ATM phosphorylation. Following γ-irradiation ATM phosphorylates ELF4, leading to its degradation; a mutant form of ELF4 that cannot be phosphorylated by ATM persists following γ-irradiation, delaying the resolution of γH2AX foci and triggering an excessive DNA damage response. Thus, although ELF4 promotes the phosphorylation of H2AX by ATM, its activity must be dampened by ATM dependent phosphorylation and degradation, to avoid an excessive DNA damage response.

### Keywords

γH2AX; Ataxia-telangiectasia mutated gene (ATM) phosphorylation; transcription factors

## Introduction

DNA damage provokes a rapid cellular response that commits cells to either repair the damaged DNA or die if the DNA damage is too great. Various stresses induce DNA breaks, which trigger local ATM activation (1) and the subsequent phosphorylation of its downstream targets, including histone H2AX (generating serine139 phosphorylated H2AX, also known as γH2AX) (2, 3), and p53 (on multiple serine/ threonine residues). In this way, activated ATM can trigger the repair of DNA by engaging a cell cycle checkpoint, or its activation can trigger the apoptosis of irreversibly damaged cells (4, 5). γH2AX is induced in response to DNA damage and it forms foci within the chromatin adjacent to the induced lesions. A number of proteins associate with γH2AX, including ATM, MDC1, 53BP1, and

Corresponding author Stephen D Nimer, MD Sloan-Kettering Institute Memorial Sloan-Kettering Cancer Center 1275 York Ave., New York, NY 10065 Phone, 646-888-3040 Fax, 646-422-0246 s-nimer@mskcc.org.

Mre11/Rad50/Nbs1 (members of the MRN complex) to initiate the DNA damage response (6, 7). While the proper regulation of the DNA damage response is critical to the life of the cell and the health of the organism, this process remains incompletely understood.

ELF4 (also known as MEF) is a member of the ETS family of transcription factors and it generally functions as a transcriptional activator (8-10). ELF4 has oncogenic properties and contributes to malignant transformation by inhibiting both the p53 and p16/Rb pathways (11, 12). ELF4 also promotes the transition of cells from G1 to S phase and enhances the movement of hemapotoietic stem cells (HSCs) out of a quiescent state (G0 phase) into the cell cycle (13, 14). The enhanced steady state quiescence of Elf4 null HSCs confers a radio-resistant and chemo-resistant phenotype to Elf4 null mice, as a non-lethal dose of γ-irradiation (4.5Gy) or treatment with 5-FU results in less leukopenia and/or faster blood count recovery compared to wild type mice (13). Elf4 null HSCs also show reduced γH2AX foci after γ-irradiation (14), suggesting a role for Elf4 in the DNA damage response.

HSCs lodge within stem cell niches that protect them from oxidative stress and other forms of DNA damage and it appears that an intact DNA damage response is critical for HSC maintenance. The absence of ATM, or an overactive ATM kinase, leads to HSC exhaustion and depletion over time (15, 16). Rad50 plays a pivotal role in sensing DNA double strand breaks (DSBs) and promoting DNA repair (17). The hypermorphic $Rad50^{S}$ variant allele constitutively activates ATM, and $Rad50^{S/S}$ mice show enhanced HSC apoptotic attrition leading to bone marrow failure at a very young age (16). This enhanced HSC apoptosis is reduced when Elf4 is absent, and $Rad50^{S/S}$/Elf4 null mice survive longer than $Rad50^{S/S}$ mice, suggesting that the absence of Elf4 reduces the $Rad50^{S/S}$-induced DNA damage response (18).

We now show that ELF4 binds to γH2AX in response to γ-irradiation, and promotes the DNA damage response, leading to apoptosis. Cells lacking Elf4 show a more rapid disappearance of detectable DNA DSBs and reduced accumulation of γH2AX leading to less p53 activation after γ-irradiation. Following γ–irradiation, ATM phosphorylates ELF4 leading to degradation of ELF4 protein; this loss of Elf4 reduces the detectable DNA DSBs, thereby diminishing the cell's apoptotic response. Expression of a mutant form of ELF4, whose degradation is not induced by ATM, results in an excessive DNA damage response to γ-irradiation via accumulating γH2AX foci. Thus, the correct timing of the appearance and disappearance of Elf4 appears to be critical for a normal cellular response to γ-irradiation.

## Materials and Methods

### Mice

Elf4 KO mice were generated as previously described (19), and the p53 KO mice and ATM heterozygous mice were kindly provided by Harold Varmus's lab, and John Petrini's lab, respectively. All mice were maintained in the MSKCC Animal Core Facility according to IACUC approved protocols. Wild type or Elf4 KO mice (3 months of age) were exposed to whole body irradiation (9Gy), and were monitored daily for survival. Prism software (Graphpad) was used to perform all statistical analyses.

### Cell lines

NIH3T3 and 293T cells were obtained from the ATCC, and possessed for less than 6 months. The cells were cultured in Dulbecco's modified Eagle's medium (DMEM) containing 10% fetal bovine serum with penicillin/streptomycin, in a humidified incubator. They were repeatedly screened for mycoplasma, and were negative.

### Cellular assays

Assays of the G1 checkpoint and the G2/M checkpoint were performed as described (20, 21). Mitotic cells were detected by staining with an anti-phospho-H3 ser10 antibody (#05-806 purchased from Millipore). The samples were analyzed by a FACScan flow cytometer (Becton-Dickinson), with FlowJo analysis software (Tree Star).

### Apoptotic assay

Mouse embryo fibroblasts were irradiated or treated with doxorubicin (0.2 μM or 0.5 μM), and incubated for 48 hours or 4 hours, respectively. Apoptotic cells were detected using a FACScan flow cytometer (Becton-Dickinson) following staining with an anti-Annexin V-PE antibody and with 7AAD (BD Biosciences).

### Comet (single cell gel electrophoresis) assay

One hour after γ-irradiation or two hours after doxorubicin treatment, cells were prepared for the CometAssay as described (Trevigen). Briefly, the cells were stained by DAPI and captured by a Zeiss fluorescence microscope. The average comet tail moment was calculated utilizing CometScore software (TriTek)

### Western blotting, immuno-precipitation, and immuno-fluorescence assays

Western blotting was performed as described (12). The primary antibodies were as follows; p53 (2524, Cell Signaling), phospho-p53 (serine18) (ab1431, Abcam), p21 (sc397, Santa Cruz), Mdm2 (ab16895, Abcam), γH2AX (2577, Cell Signaling), H2AX (DR1016, Calbiochem), phospho-ATM (ser1981) (4526, Cell Signaling), ATM (2873, Cell Signaling), phospho-(Ser/Thr) ATM/ATR substrate (2851, Cell Signaling), anti-Flag (F7425, Sigma), and α-tubulin (T9026, Sigma). Immuno-precipitation was performed as previously described (22), using cell extracts prepared in RIPA buffer with 1% Nonidet P40.

For the immuno-fluorescence assays, $8\times10^4$ mefs were seeded in 4-well chamber slides (LabTek), and one day later the cells were irradiated. 30 minutes after γ-irradiation, the cells were fixed with 4% paraformaldehyde, and permeabilized with 0.1% Triton-X. Cells were blocked with 2% FBS, and incubated with the primary antibodies as follows; anti-Elf4 rabbit polyclonal antibody as described (22), and (mouse monoclonal) anti-γH2AX (613401, Biolegend), followed by Alexa546 anti-rabbit and Alexa488 anti-mouse secondary antibodies (Molecular Probes). The cells were stained by DAPI and captured by a Zeiss fluorescence microscope.

### Plasmids and trasfections

Mutant forms of ELF4 were generated from the pCMV5 Flag-tagged ELF4 plasmid using the QuikChange II Site-Directed Mutagenesis Kit (Stratagene). Primers for the phosphorylation site mutations were as follows: threonine 70 to alanine, 5'-gggaccttgtgcatggcgcaggatcagatcc-3 and 5'-ggatctgatcctgcgccatgcacaaggtccc-3'; serine 369 to alanine, 5'-tggaattgggaccggcgctagacgaggag-3' and 5'-ctcctcgtctagcgccggtcccaattcca-3'; and serine 472 to alanine, 5'-ccagtttccaagacgcccaggtggcagccc-3' and 5'-gggctgccacctgggcgtcttggaaactgg-3'. All mutants were confirmed by DNA sequencing. The plasmids were transiently transfected into mefs using FuGENE 6 (Roche); all assays were performed 48 hours after transfection. To knock down Elf4 expression, Elf4 mRNA was expressed using the lentivirus vector pLKO.1 (Openbiosystems, Huntsville, AL), following transfection into 293T cells using a standard calcium phosphate method. The procedure performed to transduce passage 3 wild type mefs is as previously described (12).

### Real time PCR

Real time PCR was performed using either a p21 TaqMan primer (Applied Biosystems) or SYBR Green primers for Bax and Gapdh, and the 7500 Real-Time PCR System (Applied Biosystems). The primers for Bax and Gapdh were as follows; Bax, 5'-aaactggtgctcaaggccct-3' and 5'-agcagccgctcacggag-3'; Gapdh, 5'-tggcaaagtggagattgttgcc-3' and 5'-aagatggtgatgggcttcccg-3'. Gapdh was measured to provide an internal standard. All data is expressed as fold-enrichment, divided by the level of Gapdh expression.

## Results

### Elf4/Mef loss confers resistance to γ-irradiation both ex vivo and in vivo

To investigate the physiological role of Elf4 in regulating the DNA damage response, we examined the viability of Elf4 knock out (KO) murine embryonic fibroblasts (mefs) versus wild type (WT) mefs after γ-irradiation, and observed significantly more viable Elf4 KO cells than WT cells, 24 hours after 5 Gy, or 10 Gy-irradiation (Figure 1a). This difference persisted 48 hours after 5 Gy-irradiation (Figure 1b), indicating that Elf4 KO cells have a radio-resistance phenotype. We found that Elf4 KO cells had intact G1 and G2/M checkpoints after γ-irradiation (Figure S1), thus we examined whether this phenotype was due to an effect on apoptosis. We stained Elf4 KO, WT mefs and p53 KO mefs for Annexin V 48 hours after 5 Gy or 10 Gy-irradiation. While 5 Gy-irradiation was not sufficient to induce significant apoptosis in these mefs, Elf4 KO cells showed significantly fewer apoptotic cells than WT cells after 10 Gy (12.8% versus 31.7% for WT mefs, $p<0.001$) (Figure 1c). Furthermore, Elf4 KO cells contained fewer sub-G1 phase cells than WT cells 48 hours after 10 Gy-irradiation (2.8%±0.9% versus 5.0%±2.6%, $p=0.034$)(Figure 1d), and less apoptosis after 4 hours of doxorubicin treatment [13.2% versus 19.8% at a dose of 0.2 μM ($p=0.018$), and 27.0% versus 37.2%, at a dose of 0.5 μM ($p<0.001$)] (Figure 1e). Thus, the absence of Elf4 impairs the apoptotic response to DNA damaging agents ex vivo.

To further explore the in vivo radio-resistance of Elf4 null mice, we first examined their survival following a lethal dose of γ-irradiation (9 Gy). While 0 of 14 WT mice survived more than 17 days after this dose of radiation, 4 of the 12 Elf4 KO mice (33%) survived

beyond 50 days (Figure 1f). Elf4 KO mice retained approximately 10% bone marrow cellularity 8 days after receiving 9Gy-irradiation, while the WT mice did not (data not shown). Thus, the absence of Elf4 confers cellular resistance to DNA damage both ex vivo and in vivo.

### The absence of Elf4 impairs the cellular DNA damage response despite activated Atm

To further understand the radio-resistance phenotype of Elf4 KO mefs, we examined whether γH2AX was normally generated at the site of DNA double strand breaks in response to γ-irradiation (23). We evaluated γH2AX foci at 5 min, 15 min, 30 min and 60 min after 5Gy-irradiation using an anti-γH2AX antibody, and DAPI immuno-fluorescence staining. We saw no difference in γH2AX foci formation at 5 min and 15 min, however, Elf4 KO cells showed significantly fewer γH2AX foci per cell, compared to WT mefs, 30 min and 60 min after γ-irradiation [12.1±7.7 versus 22.0±9.1 for 30 min ($p<0.001$), and 6.4±6.1 versus 15.1±9.1 for 60 min ($p<0.001$)] (Figure 2a). We also evaluated the level of γH2AX expression at 5, 15, 30 and 60 min after 5Gy-irradiation by immuno blotting. Elf4 KO cells show less induction of γH2AX after γ-irradiation with peak γH2AX expression 30 min after γ-irradiation, while WT cells show continually increasing γH2AX expression over the 60 min after γ-irradiation (Figure 2b). Thus, both assays show less γH2AX in irradiated Elf4 KO cells than WT cells.

The Elf4 KO cells have higher p53 expression and lower Mdm2 expression than WT cells at baseline (Figure 2b and reference 12). Consistent with their radio-resistant phenotype, there is no increase in p53 levels within 60 min of 5 Gy-irradiation, nor is there increased Mdm2 expression (Figure 2b). We irradiated Elf4 KO cells at different doses (1 Gy, 2.5 Gy, 5 Gy or 10 Gy), and found impaired accumulation of p53, independent of dose (Figure S2). Thus, Elf4 KO cells show the more rapid disappearance of γH2AX foci, and a blunted accumulation of p53 protein in response to γ-irradiation. To further define the impaired activation of p53 in the Elf4 KO cells post γ-irradiation, we examined the expression of several p53 target genes (including p21 and Bax). While we found no difference in their expression in un-irradiated mefs, post-irradiation Elf4 KO cells showed less expression of both p21 and Bax mRNA (5.2±1.1 versus 11.8±4.5 for p21, 1.1±0.2 versus 4.6±1.9 for Bax comparing Elf4 KO to WT mefs)(Figure 2c). Thus, the absence of Elf4 impairs the activation of p53 function after γ-irradiation, indicating a role for Elf4 in the p53 pathway independent of its regulation of MDM2 expression.

To exclude the possibility that the chronic lack of Elf4 leads to a suppression of the DNA damage response due to chronic (compensatory) changes in the expression of DNA damage response pathway genes, we also acutely knocked down Elf4 in wild type mefs, using shRNA. The shRNA-transduced mefs had a 95% knockdown in Elf4 mRNA, compared to the control mefs (Figure S3). The Elf4 knock down cells had less induction of p53, phospho-p53, γH2AX and p21 expression than the control transduced cells after 5 Gy-irradiation (Figure 2d, lane 1 vs. lane 2 and lane 4 vs. lane 5). As previously noted (12), the un-irradiated Elf4 knock down cells expressed more p53 and p21 protein than the control cells (Figure 2d, lane 4 vs. lane 1). Thus, although Elf4 suppresses p53 expression in the steady

state (by directly activating Mdm2 expression), Elf4 can promote p53 function post γ-irradiation.

To show that it is the absence of Elf4 that causes the impaired DNA damage response, we re-expressed ELF4 in the Elf4 KO cells and examined the expression of γH2AX and p53 after 5 Gy-irradiation. ELF4 transduced Elf4 KO cells had increased γH2AX and p53 expression one and two hours after 5 Gy-irradiation (Figure 2e, compare lanes 2 and 3 with lanes 7 and 8). Thus, Elf4 is required for the induction of γH2AX and p53 protein expression in response to γ-irradiation.

Since both H2AX and p53 are major downstream substrates of the Atm kinase post γ-irradiation, we examined Atm auto-phosphorylation (on serine 1981)(p-Atm) in Elf4 KO and WT cells after γ-irradiation. We found no defect in p-Atm generation 30 min or 60 min after 5 Gy-irradiation (Figure 2f), indicating that Atm activation is normal in cells lacking Elf4 after γ-irradiation, even though Elf4 KO cells show no induction of p53 expression post irradiation (Figure 2b). These results suggest that Elf4 plays a critical role in both the persistence of irradiation-induced γH2AX foci and the activation of p53 that occurs following Atm phosphorylation.

### The absence of Elf4 reduces DNA double strand breaks after genotoxic stress

Given the normal activation of Atm, but more rapid disappearance of γH2AX foci and reduced apoptosis after γ-irradiation, we examined whether there are fewer DNA DSBs in the Elf4 KO murine embryonic fibroblasts. Since γH2AX localizes at sites of DNA DSBs, we performed single cell gel electrophoresis (comet) assays (24), to assess the amount of DNA double strand breaks at 15 min, 30 min, and 60 min post irradiation. While both WT and Elf4 KO cells show similar comet tail moments 15 min after 5 Gy-irradiation, Elf4 KO mefs have a much shorter comet tail 30 min and 60 min after irradiation than do WT cells [7.7±2.2 versus 22.4±5.2 for 30 min ($p=0.005$), and 4.4±4.7 versus 19.0±0.3 for 60 min ($p=0.024$)] (Figure 3a). We also examined the generation of DNA DSBs in cells treated with doxorubicin, an inhibitor of topoisomerase II and once again, the Elf4 KO cells showed significantly shorter comet tail moments after a 2 hour exposure to doxorubicin (13.7±14.3 versus 43.3±17.6 for WT mefs, $p<0.001$)(Figure 3b); this result is consistent with the reduced apoptotic response that we observed (Figure 1d). Thus, the Elf4 KO cells show reduced numbers of DNA DSBs (compared to WT mefs) after both γ-irradiation and doxorubicin exposure, implying that Elf4 loss promotes the faster repair of damaged DNA leading to a radio-resistant phenotype.

### Elf4 is recruited to the DNA damage foci with Atm and γH2AX in response to γ-irradiation

The more rapid disappearance of damaged DNA seen in the absence of Elf4 and the impaired DNA damage response leads to less p53 activation, despite the presence of activated Atm. Because γH2AX plays a key role in initiating the DNA damage response (2), we used immuno-fluorescence to examine whether Elf4 localizes to γH2AX DNA damage foci. First, we confirmed the specificity of the anti-Elf4 antibody, as we saw no detectable Elf4 staining in Elf4 KO cells (Figure S4). We observed no Elf4 or γH2AX foci in un-irradiated WT mefs, however 30 min after 5-Gy irradiation WT mefs had nuclear foci that

contained both Elf4 and γH2AX (Figure 4a). To examine the physical association between Elf4 and γH2AX in vivo, we irradiated NIH3T3 cells transduced with Flag tagged ELF4 (5Gy), and observed the co-precipitation of ELF4 and γH2AX primarily in the irradiated cells (Figure 4b). We also examined the physical association between ELF4 and ATM in vivo, and observed co-precipitation of ELF4 and phospho-Atm (serine 1981) in the irradiated, but not the un-irradiated cells (Figure 4c, bottom panel). Since ELF4 binds DNA as a transcription factor, we added DNase I to determine whether DNA is necessary for the association between ELF4 and γH2AX in vivo; we saw no effect, which indicates that this interaction does not require DNA (data not shown). Thus, ELF4 associates with γH2AX and with ATM at sites of DNA damage foci in response to γ-irradiation. This allows ELF4 to regulate the DNA damage response, impairing the repair of damaged DNA, but also optimizing the activation of p53 to trigger an apoptotic response.

### Elf4 is phosphorylated by Atm after γ-irradiation, leading to its degradation

Since ELF4 associates with phospho-ATM after γ-irradiation, we also examined whether ATM phosphorylates ELF4 in response to DNA damage. The human ELF4 protein has three consensus ATM kinase motif S/TQ sites (T70, S369, and S472) (25) (Figure 5a), and the mouse Elf4 protein two (T69, and S368). 293T cells transduced with (Flag tagged), however ELF4 were treated with caffeine (5mM), an ATM kinase inhibitor, for 15 min, and then irradiated (5Gy). Fifteen minutes later, the cell extracts were subjected to IP using an anti-Flag antibody followed by immuno-blotting with an antibody against S/TQ phosphorylation. While we did not see a difference in ELF4 phosphorylation in the un-irradiated cells, ELF4 phosphorylation increased (at S/TQ sites) in the irradiated cells, in a caffeine sensitive manner (Figure 5b, compare lanes 3 and 4), strongly suggesting that ATM phosphorylates ELF4 in response to γ-irradiation.

Atm KO mefs have higher basal levels of Elf4 protein than WT mefs (Figure 5c, shown by arrow), so we examined whether Elf4 protein stability is regulated by Atm-dependent phosphorylation following γ-irradiation. (Flag tagged) ELF4 transduced NIH3T3 cells were treated with caffeine for 15 min, irradiated (5 Gy) for 15 min, and then treated with cyclohexamide for up to 6 hours, to determine the half-life of ELF4 in the presence and absence of caffeine. Caffeine impairs the degradation of ELF4 protein after 5 Gy-irradiation (Figure 5d), suggesting that phosphorylation of ELF4 by ATM promotes its degradation after γ-irradiation.

We next examined whether the degradation of ELF4 was proteasome-dependent. We treated 5 Gy-irradiated ELF4 expressing NIH3T3 cells with the proteasome inhibitor MG132, and observed maintenance of the level of ELF4 protein 6 hours after γ-irradiation (Figure 5e). Having previously shown that ELF4 degradation can be triggered by cyclin/cdk-dependent phosphorylation at S641, T643, and S648 (26), we examined whether these sites (shown in Figure 5a) play a role in γ-irradiation induced ELF4 degradation; however the (S641A, T643A, and S648A) ELF4-3A mutant protein is rapidly and normally degraded, indicating that Atm is not acting via these sites (Figure S5). We next mutated all three consensus ATM phosphorylation site motifs in ELF4 to alanines (T70A, S369A, and S472A (ELF4-Atm3A mutant protein)), and examined its half-life after γ-irradiation. ELF4 or ELF4-Atm3A

mutant (Flag tagged) transduced NIH3T3 cells were irradiated (5 Gy) for 15 min, and then treated with cyclohexamide for 6 hours. While the half-life of the ELF4-Atm3A mutant was similar to wild type ELF4 before γ-irradiation (Figure 5f), the degradation of ELF4-Atm3A was abrogated post γ-irradiation (Figure 5f). Thus, Atm promotes Elf4 protein degradation after γ-irradiation via phosphorylation at these sites.

Given the positive effect of Elf4 on γH2AX accumulation and p53 activation, we examined whether the ELF4-Atm3A mutant further enhanced the DNA damage response to γ-irradiation. We transduced wild type ELF4 or the ELF4-Atm3A mutant into Elf4 KO mefs, and examined γH2AX focus formation 30 min after 5 Gy γ-irradiation. While 5% of the empty vector transduced cells stained positive for >20 γH2AX foci, 53% of wild type ELF4 transduced cells were positive, and 82% of the ELF4-Atm3A transduced cells were positive for >20 γH2AX foci per cell (Figure 5g). This implies that the persistence of Elf4 leads to greater formation of γH2AX foci, perhaps due to slower repair of DNA DSBs. We also observed increased phopho-p53 when the less degradable ELF4 mutant protein was expressed (data not shown). This data further suggests that ELF4 plays a key role in promoting the early phase of the cellular response to DNA damage, but its degradation influences the DNA repair process.

## Discussion

The MRN complex senses DNA damage and triggers a cascade of phosphorylation events initiated by ATM leading to γH2AX foci accumulation, which then promotes the repair of damaged DNA (4, 5). Cells lacking Elf4 show a radio- and chemo-resistant phenotype (13, 14), and we now demonstrate that ELF4 plays a novel role in modulating the DNA damage response. ELF4 participates in the resolution of γH2AX focus after γ-irradiation and doxorubicin treatment; in its absence cells display a more rapid disappearance of DNA double strand breaks and γH2AX foci after γ-irradiation. While ELF4 co-localizes with γH2AX post γ-irradiation, we have not found direct binding in vitro, which suggests that other proteins are required for this interaction to occur. The absence of Elf4 does not alter the phosphorylation of ATM after γ-irradiation although we do observe the reduced accumulation of ATM substrates, e.g. γH2AX and phospho-p53. Thus, Elf4 functions downstream of Atm activation to play a critical role in the cellular response to γ-irradiation. ATM also phosphorylates ELF4 protein on several consensus ATM S/TQ phosphorylation sites, leading to its degradation.

We found that in the absence of Elf4, cells display fewer DNA breaks (i.e. shorter comet tails and impaired accumulation of γH2AX foci) as well as a muted DNA damage response (i.e. reduced accumulation of p53), leading to less apoptosis. The γ-irradiation-induced increase in p53 function is compromised in Elf4 KO cells with impaired expression of p21 and Bax mRNA. These effects are due to the absence of Elf4 because re-expression of ELF4 restores the expression of both γH2AX and p53 in Elf4 KO cells after γ-irradiation. The ATM kinase is a key player in the DNA damage response, controlling the activity of its target proteins the MRN complex, γH2AX and p53, to promote the repair of damaged DNA. Elf4 enhances the Atm-dependent generation of γH2AX damage foci, leading to p53 dependent apoptosis post-irradiation.

The importance of the ATM-dependent degradation of ELF4 in the DNA damage response is illustrated by the behavior of Elf4 KO cells that express the ELF4-Atm3A mutant protein. In response to γ-irradiation, the ELF4-Atm3A mutant expressing cells show greater accumulation of γH2AX foci than wild type ELF4 expressing cells. Elf4 participates in the initiation phase of the Atm pathway and if not appropriately degraded, it can continue to promote Atm activity. Thus, while the absence of Elf4 promotes the faster repair of damaged DNA post γ-irradiation, its degradation in wild type cells appears to limit the DNA damage response.

We have identified a novel mechanism by which a transcription factor, ELF4/MEF, regulates the DNA damage response. We previously showed that Elf4 promotes Mdm2 expression in the steady state, leading to less p53 protein accumulation (12). However, post-irradiation, Elf4 promotes p53 function, a contrast with its role in the steady state, indicating that the regulation of p53 function by ELF4 changes dramatically under steady state versus stress conditions.

Understanding how to preserve normal cell growth while promoting the death of malignant cells in response to γ-irradiation is essential to enhancing its therapeutic efficacy. The radio-resistance and chemo-resistance of Elf4 KO murine embryonic fibroblasts (and HSCs) certainly suggests that by understanding the signaling pathways that control the triggering of DNA damage and its sensing, we will be able to design more effective treatment strategies for cancer.

## Supplementary Material

Refer to Web version on PubMed Central for supplementary material.

## Acknowledgments

We thank Dr. John Petrini for his critical reading of the manuscript, and the members of the Nimer lab for their helpful ideas and discussion. This work was supported by NIH Grant R01 DK52208 (SDN), and the Maynard Parker Leukemia Research Fund. Equipment used for these studies was funded by the Mr. William H. and Mrs. Alice Goodwin and the Commonwealth Foundation for Cancer Research, and the Experimental Therapeutics Center of MSKCC.

## References

1. Bakkenist CJ, Kastan MB. DNA damage activates ATM through intermolecular autophosphorylation and dimer dissociation. Nature. 2003; 421(6922):499–506. [PubMed: 12556884]
2. Celeste A, Petersen S, Romanienko PJ, Fernandez-Capetillo O, Chen HT, Sedelnikova OA, et al. Genomic instability in mice lacking histone H2AX. Science. 2002; 296(5569):922–927. [PubMed: 11934988]
3. Khanna KK, Keating KE, Kozlov S, Scott S, Gatei M, Hobson K, et al. ATM associates with and phosphorylates p53: mapping the region of interaction. Nat Genet. 1998; 20(4):398–400. [PubMed: 9843217]
4. Lavin MF. Ataxia-telangiectasia: from a rare disorder to a paradigm for cell signalling and cancer. Nat Rev Mol Cell Biol. 2008; 9(10):759–769. [PubMed: 18813293]
5. Shiloh Y. ATM and related protein kinases: safeguarding genome integrity. Nat Rev Cancer. 2003; 3(3):155–168. [PubMed: 12612651]

6. Lee JH, Paull TT. ATM activation by DNA double-strand breaks through the Mre11-Rad50-Nbs1 complex. Science. 2005; 308(5721):551–554. [PubMed: 15790808]
7. Uziel T, Lerenthal Y, Moyal L, Andegeko Y, Mittelman L, Shiloh Y. Requirement of the MRN complex for ATM activation by DNA damage. Embo J. 2003; 22(20):5612–5621. [PubMed: 14532133]
8. Miyazaki Y, Sun X, Uchida H, Zhang J, Nimer S. MEF, a novel transcription factor with an Elf-1 like DNA binding domain but distinct transcriptional activating properties. Oncogene. 1996; 13(8): 1721–1729. [PubMed: 8895518]
9. Hedvat CV, Yao J, Sokolic RA, Nimer SD. Myeloid ELF1-like factor is a potent activator of interleukin-8 expression in hematopoietic cells. J Biol Chem. 2004; 279(8):6395–6400. [PubMed: 14625302]
10. Lacorazza HD, Nimer SD. The emerging role of the myeloid Elf-1 like transcription factor in hematopoiesis. Blood Cells Mol Dis. 2003; 31(3):342–350. [PubMed: 14636650]
11. Yao JJ, Liu Y, Lacorazza HD, Soslow RA, Scandura JM, Nimer SD, et al. Tumor promoting properties of the ETS protein MEF in ovarian cancer. Oncogene. 2007; 26(27):4032–4037. [PubMed: 17213815]
12. Sashida G, Liu Y, Elf S, Miyata Y, Ohyashiki K, Izumi M, et al. ELF4/MEF activates MDM2 expression and blocks oncogene-induced p16 activation to promote transformation. Mol Cell Biol. 2009; 29(13):3687–3699. [PubMed: 19380490]
13. Lacorazza HD, Yamada T, Liu Y, Miyata Y, Sivina M, Nunes J, et al. The transcription factor MEF/ELF4 regulates the quiescence of primitive hematopoietic cells. Cancer Cell. 2006; 9(3): 175–187. [PubMed: 16530702]
14. Liu Y, Elf SE, Miyata Y, Sashida G, Liu Y, Huang G, et al. p53 regulates hematopoietic stem cell quiescence. Cell Stem Cell. 2009; 4(1):37–48. [PubMed: 19128791]
15. Ito K, Hirao A, Arai F, Matsuoka S, Takubo K, Hamaguchi I, et al. Regulation of oxidative stress by ATM is required for self-renewal of haematopoietic stem cells. Nature. 2004; 431(7011):997–1002. [PubMed: 15496926]
16. Morales M, Theunissen JW, Kim CF, Kitagawa R, Kastan MB, Petrini JH. The Rad50S allele promotes ATM-dependent DNA damage responses and suppresses ATM deficiency: implications for the Mre11 complex as a DNA damage sensor. Genes Dev. 2005; 19(24):3043–3054. [PubMed: 16357220]
17. Hopfner KP, Craig L, Moncalian G, Zinkel RA, Usui T, Owen BA, et al. The Rad50 zinc-hook is a structure joining Mre11 complexes in DNA recombination and repair. Nature. 2002; 418(6897): 562–566. [PubMed: 12152085]
18. Morales M, Liu Y, Laiakis EC, Morgan WF, Nimer SD, Petrini JH. DNA damage signaling in hematopoietic cells: a role for Mre11 complex repair of topoisomerase lesions. Cancer Res. 2008; 68(7):2186–2193. [PubMed: 18381424]
19. Lacorazza HD, Miyazaki Y, Di Cristofano A, Deblasio A, Hedvat C, Zhang J, et al. The ETS protein MEF plays a critical role in perforin gene expression and the development of natural killer and NK-T cells. Immunity. 2002; 17(4):437–449. [PubMed: 12387738]
20. Theunissen JW, Petrini JH. Methods for studying the cellular response to DNA damage: influence of the Mre11 complex on chromosome metabolism. Methods Enzymol. 2006; 409:251–284. [PubMed: 16793406]
21. Xu B, Kim ST, Lim DS, Kastan MB. Two molecularly distinct G(2)/M checkpoints are induced by ionizing irradiation. Mol Cell Biol. 2002; 22(4):1049–1059. [PubMed: 11809797]
22. Miyazaki Y, Boccuni P, Mao S, Zhang J, Erdjument-Bromage H, Tempst P. Cyclin A-dependent phosphorylation of the ETS-related protein, MEF, restricts its activity to the G1 phase of the cell cycle. J Biol Chem. 2001; 276(44):40528–40536. [PubMed: 11504716]
23. Rogakou EP, Pilch DR, Orr AH, Ivanova VS, Bonner WM. DNA double-stranded breaks induce histone H2AX phosphorylation on serine 139. J Biol Chem. 1998; 273(10):5858–5868. [PubMed: 9488723]
24. Olive PL, Banath JP. The comet assay: a method to measure DNA damage in individual cells. Nat Protoc. 2006; 1(1):23–29. [PubMed: 17406208]

25. Kim ST, Lim DS, Canman CE, Kastan MB. Substrate specificities and identification of putative substrates of ATM kinase family members. J Biol Chem. 1999; 274(53):37538–37543. [PubMed: 10608806]

26. Liu Y, Hedvat CV, Mao S, Zhu XH, Yao J, Nguyen H, et al. The ETS protein MEF is regulated by phosphorylation-dependent proteolysis via the protein-ubiquitin ligase SCFSkp2. Mol Cell Biol. 2006; 26(8):3114–3123. [PubMed: 16581786]

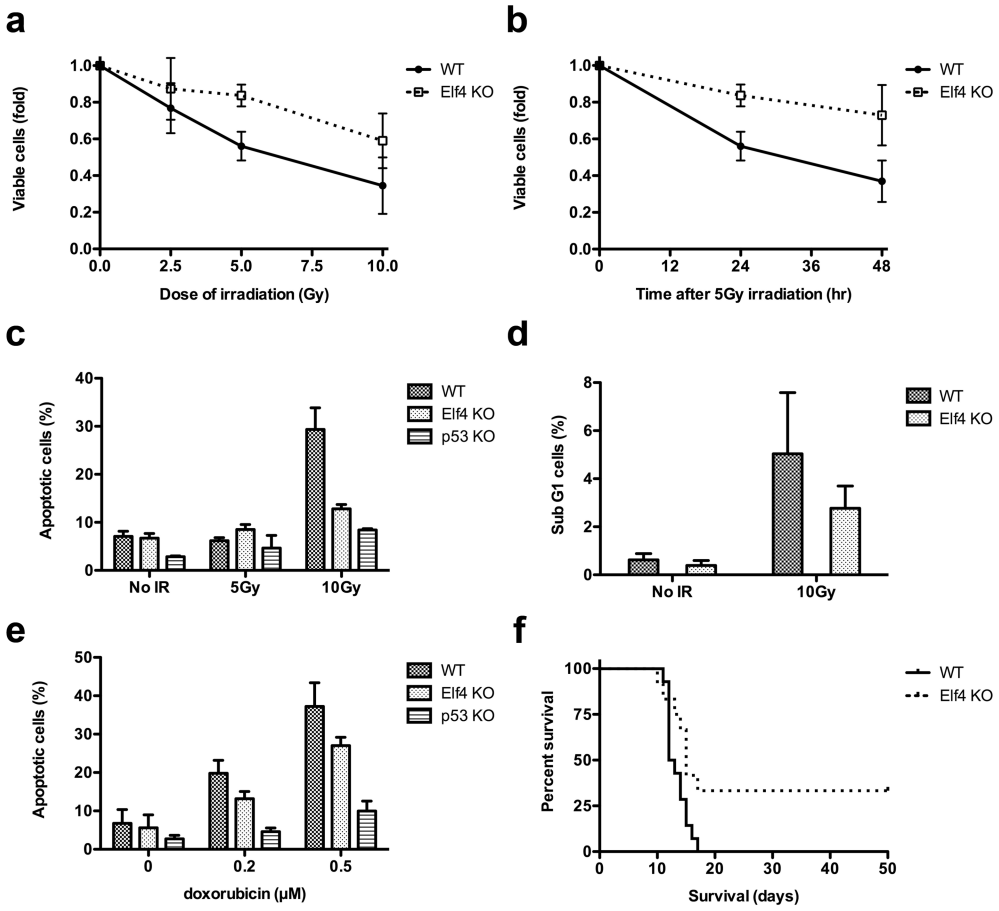


**Figure 1. Elf4 loss confers resistance to DNA damage *ex vivo* and *in vivo***

a) Elf4 KO cells show resistance to γ-irradiation. Elf4 KO and WT mefs were irradiated (2.5, 5, or 10 Gy), and the number of viable cells was measured by trypan blue exclusion at 24 hours. Elf4 KO cells showed significantly higher cell numbers (than WT mefs) after 5 Gy and 10 Gy ($p=0.0019$, and $p=0.0314$, respectively, n=4).

b) Resistance of Elf4 KO cells to γ-irradiation (5 Gy) is seen both 24 hours and 48 hours post γ-irradiation, as Elf4 KO mefs consistently show higher cell numbers than WT cells ($p=0.0019$, n=4).

c) Elf4 KO cells have a decreased apoptotic response to γ-irradiation. Annexin V positive WT, Elf4 KO and p53 KO mefs were measured by flow cytometry 48 hours after γ-irradiation (10 Gy). Elf4 KO cells showed significantly fewer positive cells than WT cells (12.8% versus 31.7%, $p=0.0001$, n=4).

d) Elf4 KO cells showed fewer sub-G1 phase cells after γ-irradiation. Elf4 KO and WT mefs were stained by propidium iodide 48 hours after 10Gy-irradiation (2.8%±0.9% versus 5.0% ±2.6%, $p=0.034$).

e) Elf4 KO cells also show resistance to doxorubicin-induced apoptosis. WT, Elf4 KO, and p53 KO mefs were treated with doxorubicin (0.2μM or 0.5μM) for 4hours, and Annexin V positive cells were measured. Elf4 KO cells showed significantly fewer positive cells than WT cells ($p=0.0177$ for 0.2 μM, and $p<0.0001$ for 0.5 μM, n=4).

f) Elf4 KO mice show greater survival in response to 9 Gy-irradiation. While none of WT mice survived more than 17 days after irradiation, 4 of 12 (33%) Elf4 KO mice survived beyond 50 days. Elf4 KO mice also showed a modestly longer median survival than WT mice (15 days versus 12.5 days, p=0.0213).

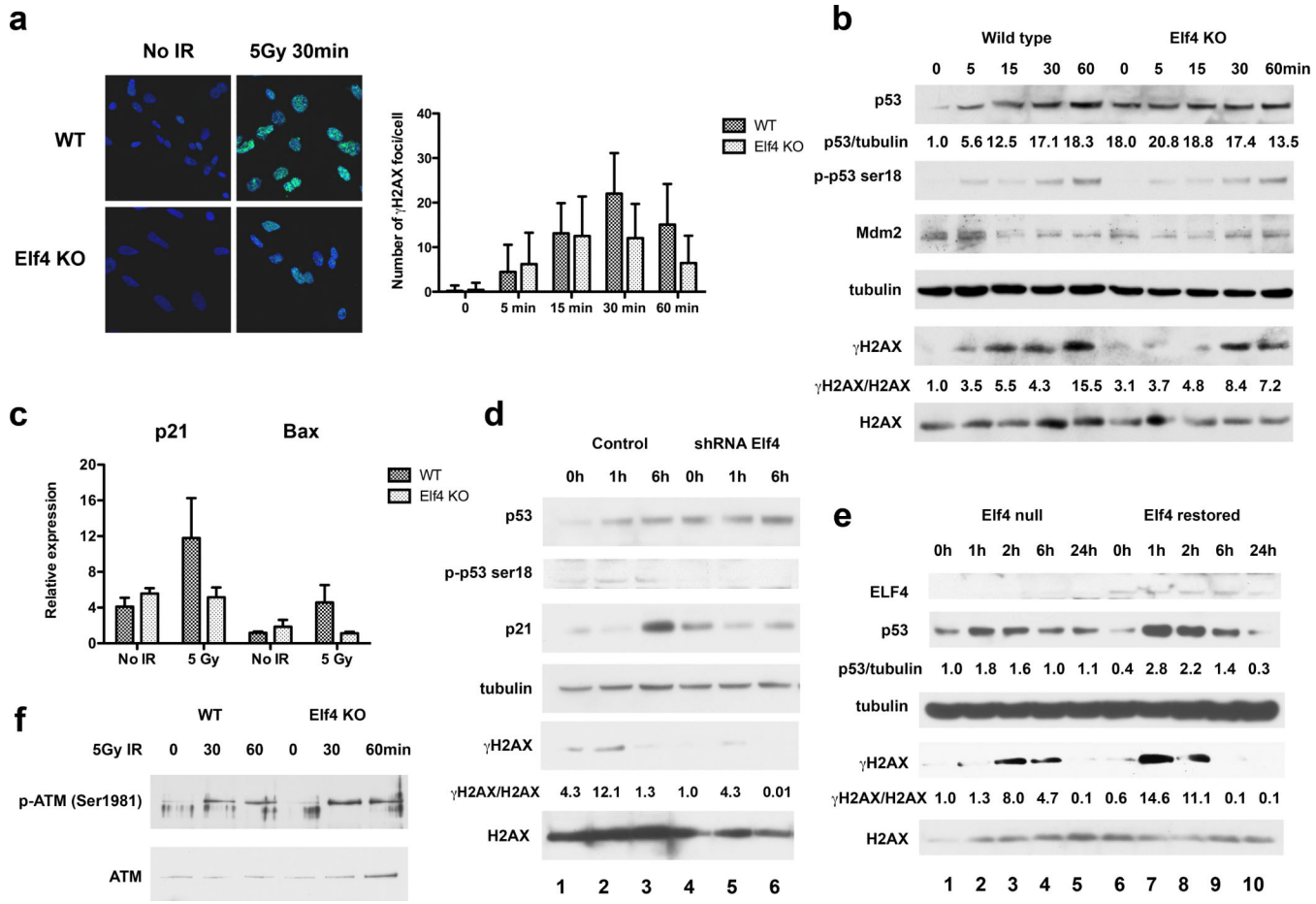


**Figure 2. The absence of Elf4 impairs the cellular DNA damage response**

a) Elf4 KO cells show a rapid reduction of γH2AX foci after γ-irradiation. Elf4 KO and WT mefs were irradiated (5Gy), and immunofluorescence was used to detect γH2AX at 5, 15, 30, and 60 min post γ-irradiation (by counting the number of γH2AX foci in each individual cell). A representative experiment is shown 30 min after 5Gy-irradiation.

b) Elf4 KO cells show less induction of p53, phospho-p53, and γH2AX after γ-irradiation. Elf4 KO and WT mefs were irradiated (5 Gy), and p53, phospho-p53 (serine18), Mdm2, and γH2AX levels were examined at 5, 15, 30 and 60 minutes by western blotting.

c) p53 target gene expression is impaired in Elf4 KO cells after γ-irradiation. Expression of the p53 target genes, p21 and Bax was examined by quantitative PCR 6 hours after 5 Gy-irradiation. Elf4 KO mefs show markedly impaired accumulation of p21 and Bax, compared to WT mefs.

d) Acute knockdown of Elf4 upregulates p53 and p21 levels and blunts the accumulation of phospho-p53 and γH2AX after γ-irradiation. The levels of p53, phospho-p53 (serine18), p21, and γH2AX were examined in the Elf4-directed shRNA and the control transduced WT cells at 0, 1, and 6 hours after 5 Gy-irradiation by western blotting.

e) Elf4 levels regulate the accumulation of p53 and γH2AX after γ-irradiation. Elf4 KO cells were transduced with either human ELF4 cDNA or control vector, and irradiated (5 Gy). ELF4 re-expression restored the accumulation of p53 and γH2AX.

f) Elf4 KO cells do not show defects in Atm activation after γ-irradiation. Elf4 KO and WT mefs were irradiated (5Gy), and Atm and phopho-Atm (at serine 1981, p-Atm) levels were examined by western blotting after 30 min and 1 hour. Similar increased expression of p-Atm was observed in both the WT and Elf4 KO cells after γ-irradiation.

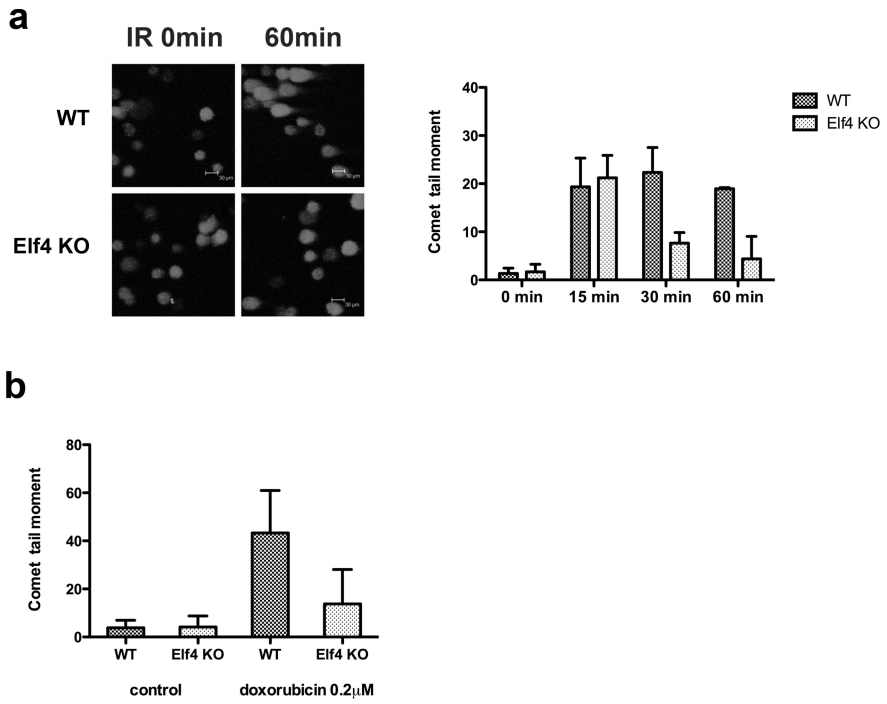


**Figure 3. The absence of Elf4 reduces DNA damaging agents-induced DNA double strand breaks**

a) Elf4 KO mefs and wild type mefs show similar comet tail moments prior to and 15 min after γ-irradiation, but Elf4 KO mefs have shorter comet tails 30 min and 1 hour after γ-irradiation. Elf4 KO and WT mefs were irradiated (5 Gy), and comet assays (single cell electrophoresis) were performed 15, 30, and 60 min post γ-irradiation. The relative comet tail moment indicate the amount of damaged DNA in a single nucleus. A representative experiment is shown, 60 min after 5Gy-irradiation.

b) Elf4 KO cells show shorter comet tails after 2 hours of doxorubicin treatment. Elf4 KO and WT mefs were treated with doxorubicin (0.2μM) for 2 hours, and the comet assay was performed.

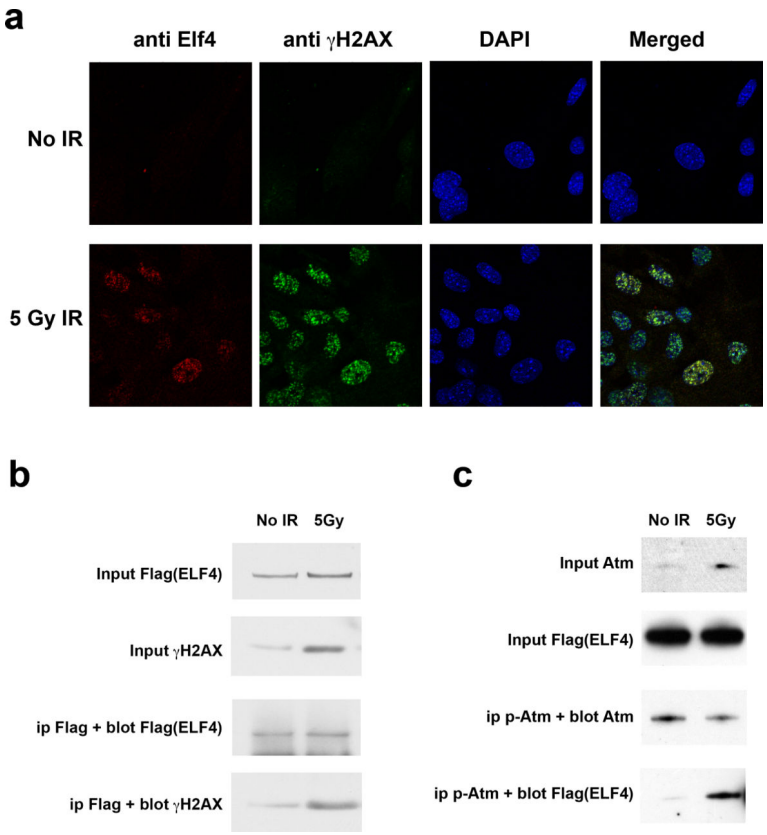


**Figure 4. Elf4 is recruited to DNA damage foci with Atm and γH2AX**

a) Elf4 protein co-localizes with γH2AX in nuclear foci after γ-irradiation. WT mefs were 5Gy-irradiated, and the cellular localization of endogenous Elf4 and γH2AX was detected by immunofluoresence after 30 min. The nuclear foci in WT mefs contain both Elf4 and γH2AX post γ-irradiation.

b) ELF4 physically associates with γH2AX *in vivo*, in response to γ-irradiation. NIH3T3 cells transduced with ELF4 (Flag tagged) were irradiated (5 Gy), and 1 hour later, cell extracts were subjected to IP using an anti-Flag antibody, followed by immunoblotting with antibodies against γH2AX or Flag. The interaction of ELF4 with γH2AX was observed in irradiated, but not un-irradiated cells.

c) Interaction of ELF4 and phospho-Atm in response to γ-irradiation. ELF4 (Flag tagged) transduced NIH3T3 cells were irradiated (5 Gy), and 1 hour later, cell extracts were subjected to IP with an antibody against phospho-Atm (at serine 1981), followed by immunoblotting with an antibody against Flag. The interaction of ELF4 with phospho-Atm was observed in irradiated, but not un-irradiated, cells.

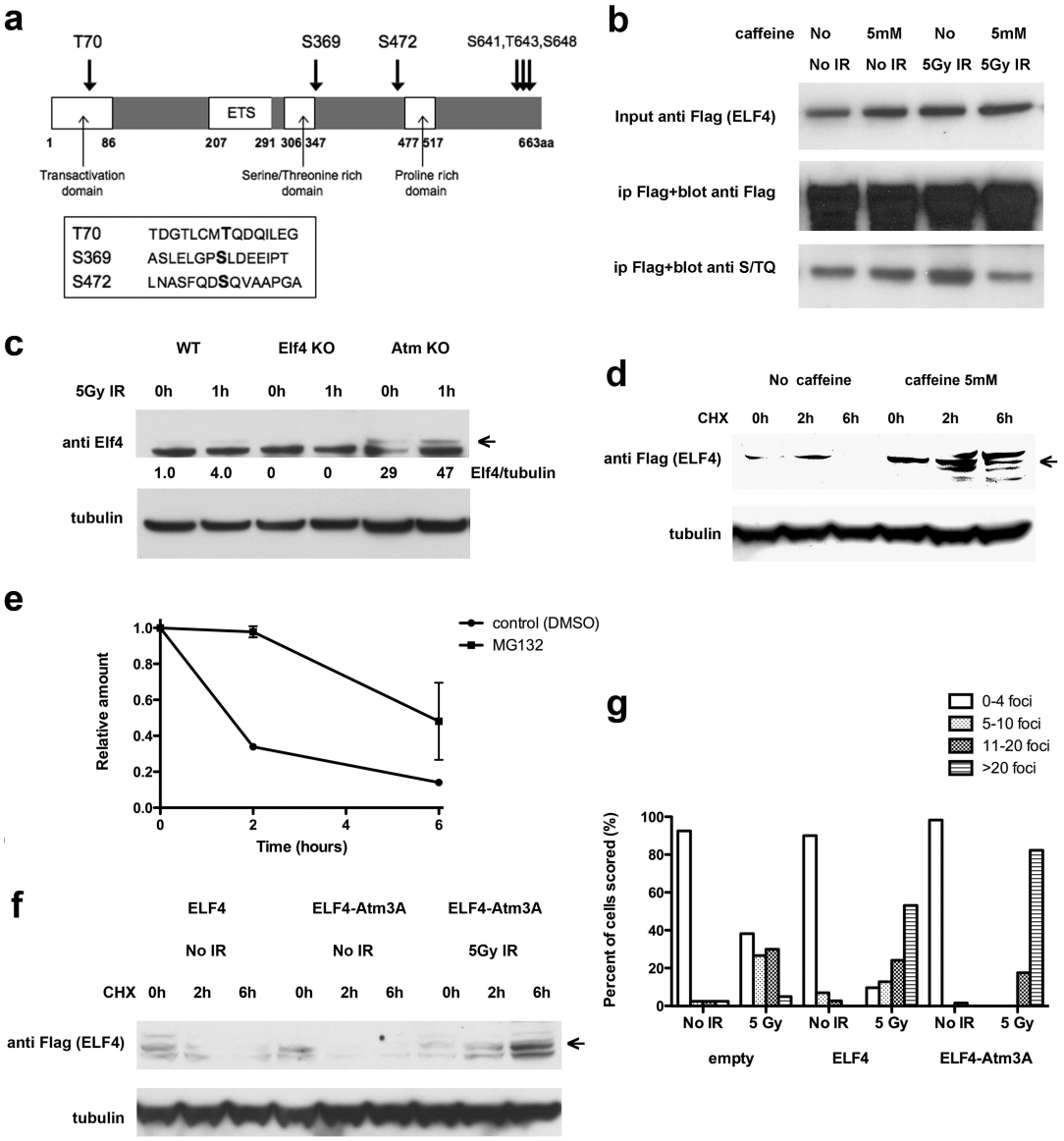


**Figure 5. ATM phosphorylates ELF4 after γ-irradiation leading to the degradation of ELF4**

a) The sites and sequences of consensus Atm kinase motifs, [S/TQ phosphorylation (T70, S369, and S472)], and the sites of C-terminal phosphorylation (S641, T643, and S648) are show in the ELF4 protein. Representative domains are also shown.

b) ELF4 is phosphorylated by Atm after γ-irradiation in vivo. ELF4 (Flag tagged) transduced 293T cells were treated with caffeine (5μM) for 15 min and irradiated (5 Gy). Fifteen minutes later cell extracts were subjected to immunoprecipitation with an antibody against Flag, followed by immunoblotting with an antibody against the phosphorylated S/TQ motif.

c) Elf4 protein accumulates in Atm KO mefs. The level of Elf4 protein was examined in WT, Elf4 KO, or Atm KO mefs 1 hour after 5 Gy-irradiation by western blotting. Elf4 KO mefs showed no detectable Elf4 protein, and WT mefs showed very low level of Elf4 expression, whereas Atm KO mefs showed higher level of Elf4 protein, which further

accumulated after irradiation (an arrow indicates the Elf4 bands, but there are non specific bands at lower size).

d) ELF4 is degraded in response to γ-irradiation in an ATM-dependent fashion. ELF4 (Flag tagged) transduced NIH3T3 cells were treated with caffeine (5μM) for 15 min, irradiated (5 Gy) for 15 min, and then treated with cyclohexamide (0.25 mM) for 6 hours. Cell extracts were prepared at 0, 2, and 6 hours post cyclohexamide treatment, and ELF4 expression was examined by western blotting using an antibody against Flag (an arrow indicates the ELF4 bands). Caffeine blocks ELF4 protein degradation after γ-irradiation.

e) ELF4 degradation is proteasome-dependent after γ-irradiation. ELF4 (Flag tagged) transduced NIH3T3 cells were treated with either the proteasome inhibitor MG132 (2μM) or DMSO, irradiated (5 Gy) for 15 min, and then treated with cyclohexamide (0.25 mM) for 6 hours. MG132 blocks ELF4 protein degradation after γ-irradiation.

f) ELF4 phosphorylation site mutations prevent its degradation in response to γ-irradiation. ELF4 or ELF4-Atm3A mutant transduced NIH3T3 cells were irradiated (mock or 5 Gy) for 15 min, and then treated with cyclohexamide (0.25 mM) for 6 hours. Cell extracts were prepared at 0, 2, and 6 hours post cyclohexamide treatment, and examined for ELF4 expression by western blotting (an arrow indicates the ELF4 bands).

g) ELF4-Atm3A enhances the formation of γH2AX foci after γ-irradiation, compared to wild type ELF4. ELF4 or ELF4-Atm3A mutant transduced Elf4 KO mefs were irradiated with 5 Gy, and 30 minutes later immuno-fluorescence was used to detect γH2AX (by counting the number of γH2AX foci in each individual cell).